A modified Three point bend specimen

Kjell Eriksson[1,a]

[1]Dept. of Solid Mechanics, Luleå University of Technology, SE 97187 Luleå, Sweden

[a]kjell.eriksson@ltu.se

Keywords: bend specimen, tapered.

Abstract. Steel profiles, such as angle sections in beams and girders, with slightly tapered cross section sides are not uncommon in older structures. Further, the fracture toughness of older and inhomogeneous steels varies in general across the thickness of a sample. The thickness of a machined, standard parallel-sided specimen of a tapered sample is in practice seldom more than 60-70 % of the full sample thickness and such a specimen captures in general inferior core material only. In view of this conundrum, a modified three point bend specimen with partly tapered sides has been designed so as to accommodate tapered samples. The project includes calibration, testing and evaluation of the modified specimen. The part of the project, which is reported here, is part analytical and part numerical and aimed at calculation of the stress intensity factor for various crack lengths, taper and specimen cross section proportions.

Introduction

Fracture mechanics is today frequently used in fitness for purpose assessments of structures of older steels, whose toughness properties often are unknown. The most common test specimen type in present assessment work is the three-point bend specimen, which is plane-parallel and of constant thickness, while common types of profiles in older structures, such as angle sections in beams and girders, often have slightly tapered sides. Samples taken from such profiles are presently machined plane-parallel and it is not uncommon that all original sample surfaces are removed. The thickness of a machined specimen is therefore, in practice, only 60-70% of the original sample. As the toughness of the surface material generally is superior, an unfairly low toughness might then be obtained for older and inhomogeneous steels.

In the present project the standard three-point bend specimen, as given in ASTM E-1820 [1], is modified so as to accommodate steel samples with tapered sides. The modified specimen allows determination of a fair effective toughness since the full sample thickness is included. In particular, the surface material of generally superior toughness is retained. Preserving the surface material in testing has often been found critical in practice.

The cross section of the modified specimen, inscribed in a typical tapered profile, is shown in Fig. 1. The project comprises development, calibration and testing of the modified specimen, including derivation and verification of expressions of the stress intensity factor K_I and the J-integral as functions of relevant parameters. The part of the project which is reported here, is part analytical and part numerical and is aimed at obtaining the stress intensity factor as influenced by the modified geometry.

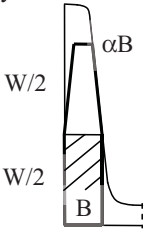

Figure 1. Cross section of modified three point bend specimen. W is specimen height, B specimen thickness of the bottom half and αB thickness at the top of the specimen.

Stress intensity factor estimation

To get an estimate of the effect of the modified geometry on the stress intensity factor, the method by Kienzler and Herrmann [2, 3, 4] to obtain approximate Mode I stress intensity factors in cracked beams has been used. These authors have shown that very simple and close approximations can be obtained with elementary bending theory [4]. For pure bending of an edge cracked beam Bazant [5] showed that the accuracy of the stress intensity factor estimation was improved by introducing a known factor of proportionality. Gao and Herrmann [6] then showed that the correction factor could be determined through matching with standard limiting crack length solutions. The method of Kienzler and Herrmann has later been used by many others, e.g. [7-9]. In this work the original method of Kienzler and Herrmann [4] is exploited to obtain a close approximation of the stress intensity factor for both the original and the modified three point bend specimen. No improvement over existing methods is obtained, but, the present procedure offers a convenient treatment of the modified geometry.

The three point bend specimen

The stress intensity factor for the three point bend specimen is obtained from [10]

$$K_I = \left(-\frac{\lambda E}{B} \frac{dU}{db}\bigg|_{b=0} \right)^{1/2} \tag{1}$$

where λ is a factor of proportionality to be determined, E Young's modulus, B specimen thickness, b one half of the width of the crack and U the potential energy. For controlled loading condition $U = -W$, where W is the specimen strain energy, which according to elementary beam theory is

$$W = 2\left[\int_0^b \left(\frac{M(x)^2}{2EI^*} + \beta \frac{T(x)^2}{2GA^*} \right) dx + \int_b^{S/2} \left(\frac{M(x)^2}{2EI} + \beta \frac{T(x)^2}{2GA} \right) dx \right] \tag{2}$$

in standard notation. For the standard three-point bend specimen the stress intensity factor is

$$K_I = 4 \frac{P}{BW^{1/2}} f_e(a/W) \tag{3}$$

$$f_e(a/W) = \left\{ \frac{\lambda}{32} \left[24 \left(\frac{1}{(1-a/W)^3} - 1 \right) + \beta(1+\nu) \left(\frac{1}{1-a/W} - 1 \right) \right] \right\}^{1/2} \tag{4}$$

where $f_e(a/W)$ is a dimensionless geometry function.

In pure bending of a single edge notched beam Bazant [5] obtained $\lambda = 1.32$. The parameter λ can alternatively be obtained through comparison with a known geometry function. The function

$$\lambda(a/W) = \frac{0.9017}{\sqrt{0.0366 + a/W - 0.0297(a/W)^2 - 0.6037(a/W)^3}} \tag{5}$$

which has been obtained by matching Eq. (4) to the standard ASTM geometry function for the three point bend specimen, using a third order least square approximation, is a close fit, within less than

0.5 % from the ASTM values for all crack lengths. In Fig. 2 is shown the geometry function Eq. (4) and the function $\lambda(a/W)$ according to Eq. (5).

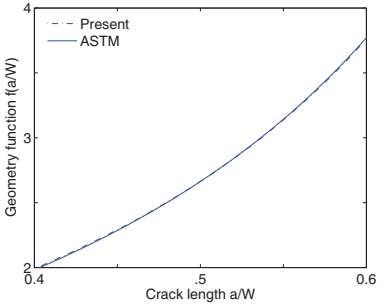

Figure 2a. Geometry functions of the stress intensity factor for the standard three-point bend specimen.

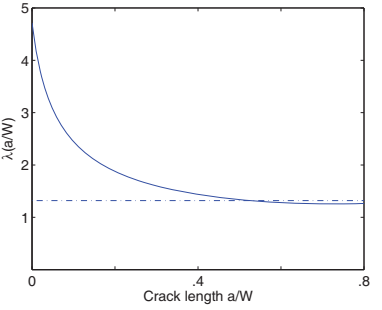

Figure 2b. The function $\lambda(a/W)$ in the Present solution. The dash-dotted line shows λ =1.32.

The modified three-point bend specimen

The cross section of the modified three point bend specimen has partly tapered sides, Fig. 3a.

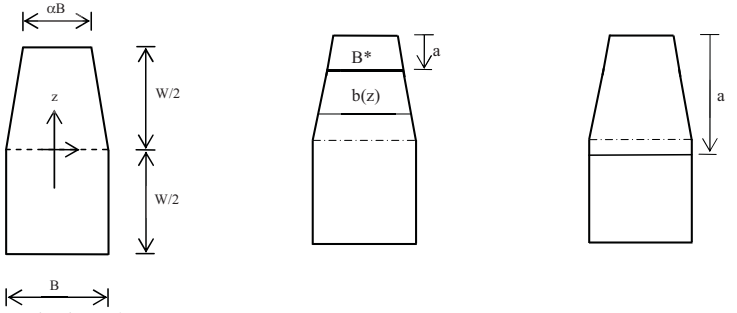

a) uncracked section b) $0 \le a/W \le 0.5$ c) $0.5 \le a/W \le 1.0$

Figure 3. Three point bend specimen with partly tapered cross-section. $\alpha \le 1$ is a dimensionless shape factor.

Cross section data/characteristics

A* and I*. The cracked section is dealt with in two parts, depending on crack length. In the crack length range $0 \le a/W \le 0.5$, Fig. 3b, the length of the crack front is

$$B^* = (b^*)B = [1-(1-2a/W)(1-\alpha)]B \tag{6}$$

where (b^*) denotes a non-dimensional part of *B**, etc., and the cross section area of the ligament (the area under *B** in Fig. 3b).

$$A^* = \{2+[2-(1-2a/W)(1-\alpha)](1-2a/W)\}\frac{BW}{4} = (A^*)\frac{BW}{4} \tag{7}$$

The moment of inertia of the ligament is

$$I^* = \frac{BW^3}{96} + \frac{BW}{2}(t - \frac{W}{4})^2 + I_1 + A_1\left(\frac{W}{2} + t_1 - t\right)^2 = (I^*)\frac{BW^3}{96} \tag{8}$$

$$t = \frac{1 + [1 + (t_1)][(A_1)}{A^*}\frac{W}{2} = (t)\frac{W}{2} \tag{9}$$

$$t_1 = (1 - 2a/W)\frac{3 - 2(1 - 2a/W)(1 - \alpha)}{3[2 - (1 - 2a/W)(1 - \alpha)]}\frac{W}{2} = (t_1)\frac{W}{2} \tag{10}$$

$$A_1 = [2 - (1 - 2a/W)(1 - \alpha)][(1 - 2a/W)\frac{BW}{4} = (A_1)\frac{BW}{4} \tag{11}$$

$$I_1 = (1 - 2a/W)^3\frac{[(3 - 2(1 - 2a/W)(1 - \alpha))]^2 - 3[(1 - (1 - 2a/W)(1 - \alpha))]^2}{2 - (1 - 2a/W)(1 - \alpha)}\frac{BW^3}{8 \cdot 36} = (I_1)\frac{BW^3}{288} \tag{12}$$

In particular, for zero crack length, $(a = 0)$, the total cross section area is

$$A = BW\, f_A(\alpha) \quad f_A(\alpha) = \frac{3 + \alpha}{4} \tag{13}$$

and the moment of inertia of the total cross section is

$$I = \frac{BW^3}{12} f_I(\alpha) \quad f_I(\alpha) = 1 + \frac{4}{3}\left(\frac{1 - \alpha}{3 + \alpha}\right)^2 - \frac{1 - \alpha}{24}\left(1 + \frac{128}{(3 + \alpha)^2}\right) \tag{14}$$

For the remainder of the cracked section, Fig. 3c, the crack length range is $0.5 \le a/W \le 1.0$, and A^* and I^* in this range are given by

$$A^* = B(W - a) \quad I^* = \frac{B(W - a)^3}{12} \tag{15}$$

Coefficient β. The coefficient β in Eq. (2) is a function of the cross-section shape. Its derivation comprises several steps and the point of departure is the bending shear stress

$$\tau^{\pm}(z) = \frac{T\, S(z)}{I\, b(z)} = \mu^{\pm}(z)\frac{T}{A^*} \tag{16}$$

where $S(z)$ is the static moment of the part of the cross-section considered, with respect to the centre of gravity of the entire cross-section, and $b(z)$ specimen thickness. The dependence on the taper parameter α of $S(z)$, I and $b(z)$ is implicit. In the crack length range $0 \le a/W \le 0.5$ the shear stress is obtained from

$$\mu^{+}(z) = 3\frac{(A^*)(A'')(t_p)}{[1 - (1 - \alpha)2z/W][I^*)} \tag{17}$$

$$A'' = [2-(1-\alpha)(1-2a/W+2z/W)](1-2a/W-2z/W)\frac{BW}{4} = (A'')\frac{BW}{4} \tag{18}$$

$$t_p = [1+2z/W+(t'')-(t)]\frac{W}{2} = (t_p)\frac{W}{2} \tag{19}$$

$$t'' = (1-2a/W-2z/W)\frac{3-2(1-\alpha)(1-2a/W+z/W)}{3[2-(1-\alpha)(1-2a/W+2z/W)]}\frac{W}{2} = (t'')\frac{W}{2} \tag{20}$$

and in the crack length range $0.5 \le a/W \le 1.0$ from

$$\mu^-(z) = 3\frac{(A^*)(A')(t')}{(I^*)} \tag{21}$$

$$A' = (1+2z/W)\frac{BW}{2} = (A')\frac{BW}{2} \tag{22}$$

$$t' = [2(t)-2z/W-1]\frac{W}{4} = (t')\frac{W}{4} \tag{23}$$

The strain energy density due to shear is $\overline{W} = \tfrac{1}{2}\tau\gamma$, where τ and γ are shear stress and strain, respectively. Using Hooke's law on the form $\tau = G\gamma$, the total strain energy per unit length of the tapered and cracked beam can be written

$$W = \frac{1}{2G}\left[\int_{-W/2}^{0}\tau^-(z)^2\,B\,\mathrm{d}z + \int_{0}^{a}\tau^+(z)^2\,b(z)\,\mathrm{d}z\right] \tag{24}$$

where $\tau^{\pm}(z)$ are given by Eqs. (16) - (23) and

$$b(z) = [1-(2z/W)(1-\alpha)]B \tag{25}$$

Introducing the dimensionless variable $\zeta = 2z/W$, Eq. (24), after substitution of Eqs. (17) - (23) and (25), can be written

$$W = \frac{1}{2G}\frac{T^2}{A^{*2}}\frac{BW}{2}\left[\int_{-1}^{0}\mu^-(\zeta)^2\,\mathrm{d}\xi + \int_{0}^{1-2a/W}\mu^+(\zeta)^2\,b(\zeta)\,\mathrm{d}\zeta\right] \tag{26}$$

The coefficient β is defined by the expression

$$W = \beta\frac{T^2}{2GA^*} \tag{27}$$

In Eq. (26), $\frac{BW}{2} = 2\frac{A^*}{(A^*)}$, and we get for β, which is a function of taper and crack length,

$$\beta = \beta(\alpha, a) = \frac{2}{(A^*)}\left[\int_{-1}^{0} \mu^-(\zeta)^2 \, \mathrm{d}\xi + \int_{0}^{1-2a/W} \mu^+(\zeta)^2 \, b(\zeta) \, \mathrm{d}\zeta\right] \tag{28}$$

This expression has been evaluated numerically according to the midpoint trapezoid integration rule and is shown graphically in Fig. 4. It is noted that for zero crack length $\beta(\alpha,0)$ is an almost linear function of α but $\beta(\alpha,a)$ is far from linear in a. As expected, for a rectangular cross section $\beta(1,a) = 1.2$ irrespective of crack length. The effect of taper upon the shear strain energy coefficient is rather weak, at the lower limit of the range of interest, or α = 0.5 and crack length $a/W \approx 0.4$, the coefficient β is some 96 % of the value for a rectangular cross-section.

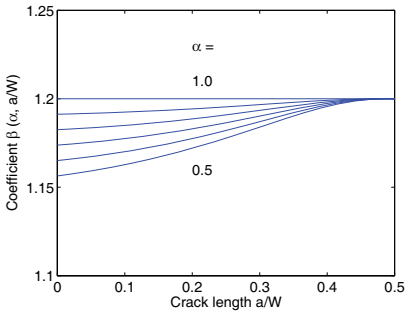

Figure 4. Shear strain energy coefficient β versus crack length and taper. $\alpha = 0.5, 0.6 \ldots 1.0$ down upwards.

Stress intensity factor

The geometry function of the stress intensity factor is now obtained by substitution of Eqs. (6) - (15) and (28) in (4) and simplification, for $0 \le a/W \le 0.5$

$$f_e(a/W) = \left\{\frac{\lambda(a)}{32(b^*)}\left[24\left(\frac{8}{(I^*)} - \frac{1}{f_1(\alpha)}\right) + (1+\nu)\left(\frac{4\beta(\alpha,a)}{(A^*)} - \frac{\beta(\alpha,0)}{f_A(\alpha)}\right)\right]\right\}^{1/2} \tag{29}$$

with $\lambda(a)$ according to Eq. (5) and for $0.5 \le a/W \le 1.0$

$$f_e(a/W) = \left\{\frac{\lambda}{32}\left[24\left(\frac{1}{(1-a/W)^3} - \frac{1}{f_1(\alpha)}\right) + (1+\nu)\left(\frac{\beta}{1-a/W} - \frac{\beta(\alpha,0)}{f_A(\alpha)}\right)\right]\right\}^{1/2} \tag{30}$$

where now λ =1.32.
In Fig. 5 is shown the normalised geometry functions for the modified specimen type, obtained from Eqs. (29) and (30), with taper in the range $0.5 \le \alpha \le 1$.

Numerical

The stress intensity factor along the crack front has been calculated numerically for specimen thicknesses $B = W/4$ and $W/2$, crack lengths a/W = 0.4, 0.5, 0.6 and taper α = 0.5 and 1.0, in all twelve different cases. A general, 3D finite element program, ANSYS® 11.0, with the options linear elastic material model, 20-node elements and small-strain deformation theory, was used. Due to two perpendicular planes of symmetry, only one quarter of the three point bend specimen was modelled and the total number of elements in the finite element mesh was of the order 21000. The element

size is varying: the smallest elements appear in the crack tip region and their size is of the order 0.003 times the crack length. Standard singular elements were used at the crack tip. Different crack lengths were obtained by shifting a fixed mesh region around the crack front and by stretching elements crack-length-wise outside this region. The shifted region is centred at the crack tip and its radius approximately $0.1W$. An example of the stress intensity factor along the crack front is shown in Fig. 6, for cross section proportions $B = W/2$, crack length $a/W = 0.5$ and taper $\alpha = 0.5$ and 1.0. The results for all cases considered are summarised in Table 2. For comparison, also the results of the 2D estimation are shown.

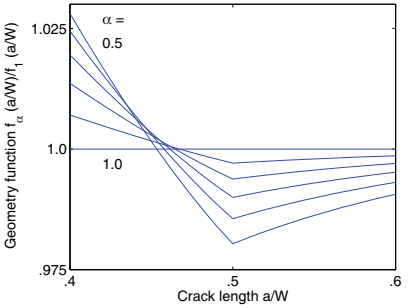

Figure 5. Normalised geometry function of the stress intensity factor for the modified three point bend specimen. $\alpha = 0.5, 0.6 \ldots 1.0$ top down to the left.

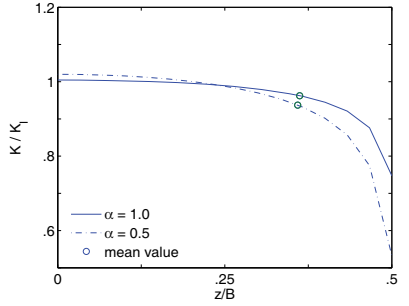

Figure 6. Influence of taper α upon normalised stress intensity factor, K/K_I, along the crack front.

Table 2. Influence of taper upon normalised stress intensity factor K/K_I.

		Taper $\alpha = 1.0$			$\alpha = 0.5$		
		3D fem		2D est	3D fem		2D est
	$a/W =$	max	mean		max	mean	
$B = W/4$	0.4	1.020	0.991	1.004	1.060	1.011	1.032
	0.5	1.018	0.978	1.000	1.019	0.968	0.981
	0.6	1.020	0.986	0.997	1.018	0.984	0.988
$B = W/2$	0.4	1.017	0.984	1.004	1.072	1.001	1.032
	0.5	1.014	0.979	1.000	1.028	0.956	0.981
	0.6	1.014	0.975	0.997	1.016	0.973	0.988

In Fig. 6 and Table 2 are shown the calculated stress intensity factor K normalised against the corresponding ASTM stress intensity factor K_I. In the 3D case, there are essentially three effects of taper upon the stress intensity factor a) the maximum value, at the centre of the specimen, is slightly increased, some 2 %, b) the mean value is slightly reduced, some 2 % and c) the minimum value at the specimen surface is reduced to a much larger extent. In the 2D case the estimated value of the stress intensity factor is slightly reduced by the taper, Fig. 6. The reduction is of the order 2% and is in close agreement with the reduction of the mean value of the 3D calculation. The slight increase of the maximum value of the stress intensity factor at the specimen centre and the larger reduction at the specimen surface are not reflected by the 2D estimation. The influence of taper upon the stress intensity factor is, on the whole, however very small, within some few percent, in all cases considered. In view of this, the 2D estimation procedure to obtain the stress intensity factor for a tapered specimen is judged to yield sufficient accuracy in practice, in particular as other uncertainties might well cause much greater errors.

References

[1] ASTM E-1820-01. Standard Test Method for Measurement of Fracture Toughness. General Book of ASTM Standards, Sect. 3, ASTM, Philadelphia (2001).

[2] G. Herrmann and H. Sosa: Engng. Fract. Mech. Vol. 24 (1986) p. 889-896.

[3] R. Kienzler and G. Herrmann: Acta Mech. Vol. 62 (1986) p. 37-46.

[4] R. Kienzler and G. Herrmann: J. Appl. Mech. Vol. 53 (1986) p. 561-564.

[5] Z.P. Bazant: Engng. Fract. Mech. Vol. 36 (1990) p. 523-525.

[6] H. Gao and G. Herrmann: Engng. Frac. Mech. Vol. 41 (1992) p. 523-525.

[7] M.L. Dunn, W. Suwito and B. Hunter: Engng. Fract. Mech. Vol. 57 (1997) p. 609-615.

[8] Y.J. Xie, P.N. Li and H. Xu: Engng. Fract. Mech. Vol. 59 (1998) p. 399-402.

[9] P. Ricci and E. Viola: 2006. Engng. Fract. Mech. Vol. 73 (2006) p. 91-111.

[10] K. Eriksson: in Experimental Analysis of Nano and Engineering Materials and Structures, edited by E.E. Gdoutos, Springer (2007).